Electronic Supplementary Information (EIS):

In situ construction of dual-functional Ni/Ni$_x$B catalysts for the hydrogenation and dehydrogenation of magnesium hydride

Hui Liang [a*], *Wenjiang Li* [b], *Jie Zheng* [c*]

[a] Institute of Material and Chemical Engineering, Xuzhou university of technology, Xuzhou 221018, China

[b] Institute for New Energy Materials & Low-Carbon Technologies and Tianjin Key Lab of Photoelectric Materials & Devices, School of Materials Science and Engineering, Tianjin University of Technology, Tianjin 300384, China

[c] Beijing National Laboratory for Molecular Sciences (BNLMS), College of Chemistry and Molecular Engineering, Peking University, Beijing 100871, China

E-mail:huiliang@xzit.edu.cn, liwj@tjut.edu.cn, zhengjie@pku.edu.cn

1. Experimental Section

1.1 Chemicals

Nickel acetylacetonate [$Ni(acac)_2$, 200 nm], sodium hydroxide (NaOH), anhydrous ethylene glycol (H_2O < 5 ppm), h-BN nanosheets (200 nm), polyethyleneimine, and anhydrous tetrahydrofuran (THF, 99.5%, H_2O < 50 ppm) were purchased from Biochemical Technology Co., Ltd.

1.2 Preparation of $Ni/Ni_xB@MgH_2$

First, 0.1 g NaOH and 30 mL distilled water were stirred and ultrasonically treated at 70°C for 6 h. Ethylene glycol was added to h-BN and stirred at 160°C for 40 min, and the precipitate was obtained by centrifugation. Subsequently, 10 mL polyethyleneimine was added to h-BN and processing by high-speed ball milling. The grafted h-BN was added to a round-bottom flask along with 0.5 g $Ni(acac)_2$ and 30 mL THF. The mixture was stirred, dried, and heated to 1,200°C. The mixture was maintained at this temperature for 90 min in Ar to obtain Ni/Ni_xB. The following samples were prepared for characterization: sample 1, ratio of h-BN to Ni^{2+} = 10:1; sample 2, h-BN: Ni^{2+} = 10:3; sample 3, h-BN: Ni^{2+} = 10:5; sample 4, h-BN: Ni^{2+} = 10:7; and sample 5, h-BN: Ni^{2+} = 1:1. Finally, Ni/Ni_xB and MgH_2 were subjected to high-speed ball milling to prepare the $Ni/Ni_xB@MgH_2$ composite. For the gas adsorption measurement, sample 1, the ratios of h-BN to Ni^{2+} : 10:1; sample 2, the ratios of h-BN to Ni^{2+}:10:3, and sample 3, the ratios of h-BN to Ni^{2+}:10:5. For fourier-transform infrared characterization, the h-BN nanosheets were grafted with different concentration ratios of OH to $-CONH_2$:Ni^{2+}/h-BN-1, OH:-$CONH_2$=10:1; Ni^{2+}/h-BN-2, -OH:-$CONH_2$=10:3; Ni^{2+}/ h-BN-3, OH:-$CONH_2$=10:10.

1.3 Characterization

X-ray diffraction (XRD) was conducted with a scanning speed of 10°/min and scanning range of 5° to 90° in increments of 0.02°. The samples were also characterized by field-emission scanning electron microscopy and aberration-corrected scanning transmission electron microscopy (STEM). The surfaces of

the samples were analyzed by X-ray photoelectron spectroscopy (XPS) using a Thermo Scientific K-alpha XPS system. Fourier-transform infrared (FTIR) spectra were obtained using a FTIR/STA6000-TL9000 MS system in the range of 4,000–400 cm^{-1}. The specific surface areas and pore size distributions of the samples were analyzed by Brunauer–Emmett–Teller (BET) surface area analysis. The N_2 absorption performances of the composites were evaluated by measuring the sorption isotherms at −196°C.

1.4 Hydrogen storage performance measurements

These Ni/Ni_xB@MgH_2 composites contain materials that adsorb H_2 through both physical and chemical absorption. High-pressure sorption equipment was used to measure the isothermal hydrogen absorption/desorption performance of the samples under constant temperature and varying pressure. PCT hydrogen equipment combined with a hydrogen generator and gas chromatography was used to analyze the kinetics of physical and chemical adsorption. PCT was explained that the high-pressure gas analysis system controlled by a computer for fully automatic operation can accurately determine the adsorption capacity of various materials such as powders and block solids for high-pressure gas. Its testing execution standard is GB19560-2008 "High pressure Isothermal Adsorption Test Method for Coal".

2. Figures and Tables

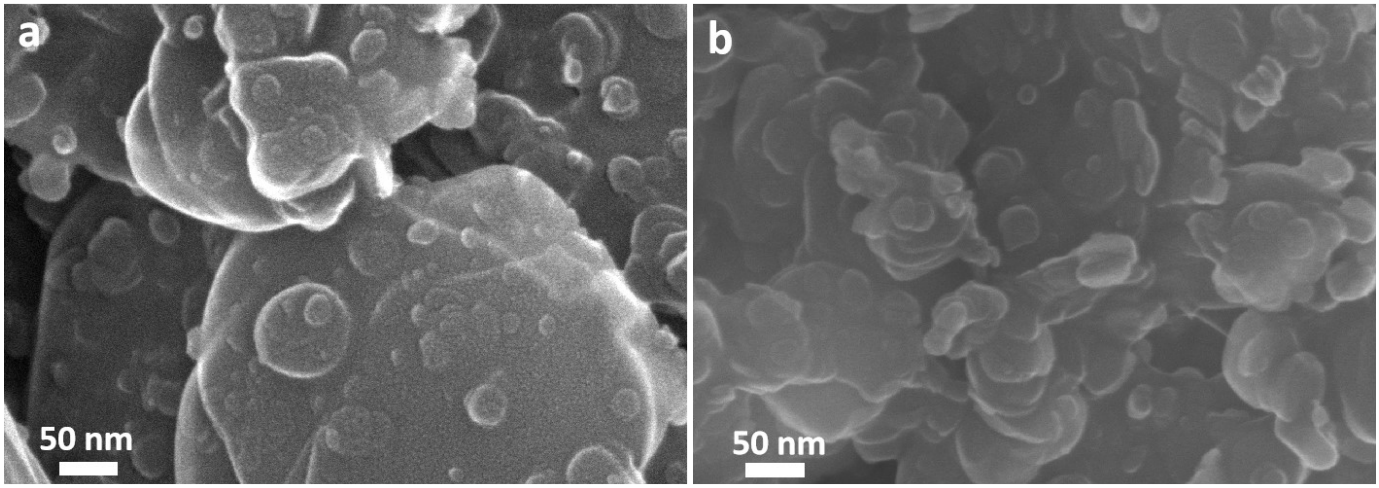

Fig. S1. The corresponding HAADF-STEM image of Ni/Ni_xB@MgH_2 composite (a), (b).

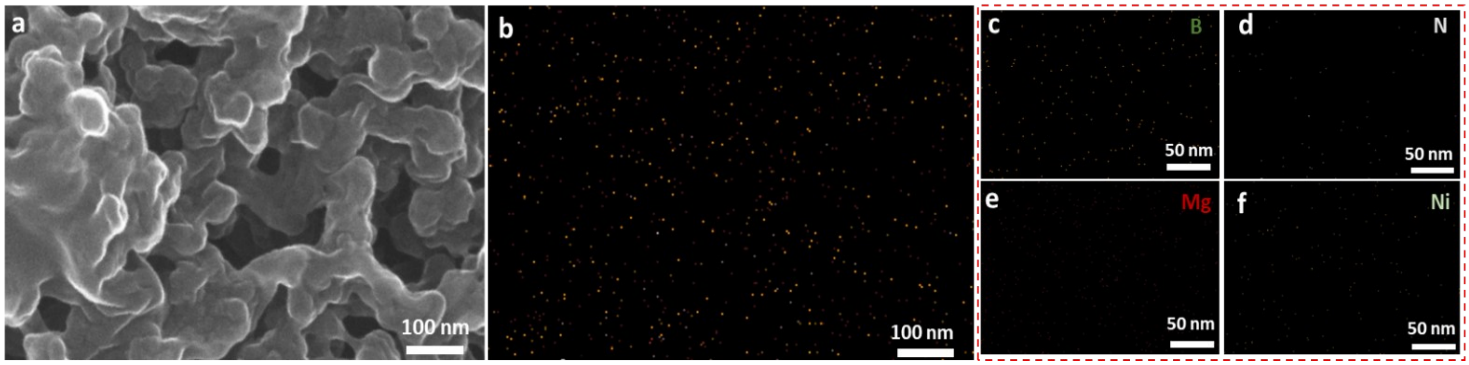

Fig. S2. SEM images of as-prepared multilayer Ni/Ni_2B/Ni_4B_3@MgH_2 composite (a). (b) EDS mapping of the corresponding B (c), N (d), Mg (e) and Ni (f).

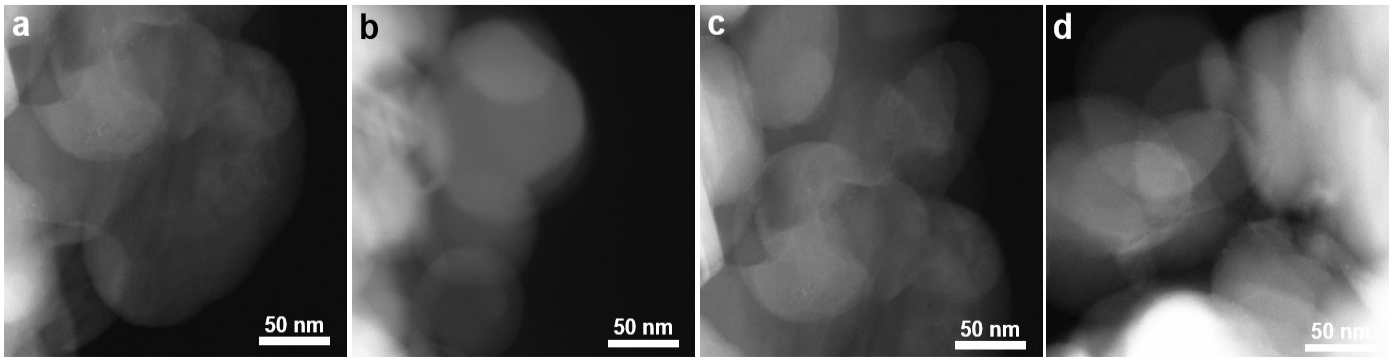

Fig. S3. The corresponding HAADF-STEM image of Ni/Ni_xB composites with different ratio of Ni^{2+} to h-BN (a), (b), (c), (d).

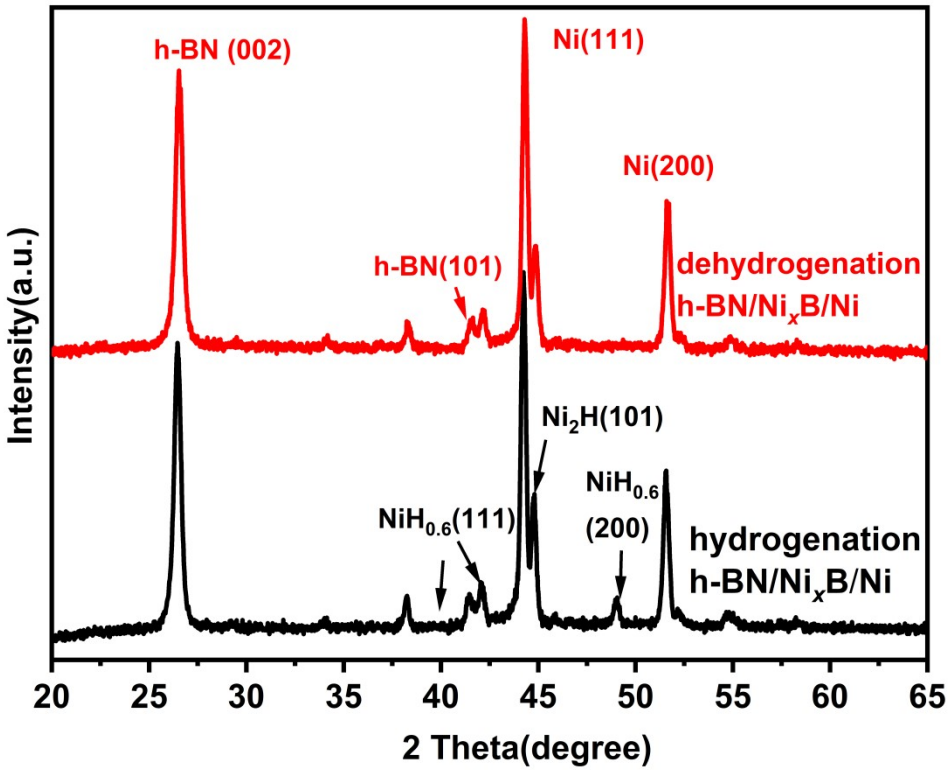

Fig.S4. The XRD spectrum of multilayer Ni/Ni$_x$B catalyst after hydrogenation and dehydrogenation (b).

Table S1. Hydrogen storage capacity and temperature of Mg-based catalysts previously reported in the literature.

Materials	Observed storage capacity (wt%)	Operation temperature (°C)
Mg_2Ni[S1]	3.4~3.6	＞327
MgH_2-LiNH[S2]	4~6	＞227
$Mg(BH_4)_2$[S3, S4]	2~3	＞300
$MgNi_XM_{0.03}$ (M=Cr, Fe, Co,Mn)[S5-S7]	3.0~3.9	＞327
$Mg(BH_4)_2(NH_3)_2$[S8]	3~5	＞227
Pt doped Mg_2Ni [S9]	6~7	＞227
Ti doped Mg_2Ni[S6,S7]	2~3	＞227
Mg-PMMA [S10]	4.5~5.5	＞327
La doped Mg_2Ni[S11]	3~5	＞277
Mg-RE[S7]	3~5	＞327
Ni@Mg[S12]	7.5%	260
Ni/h-BN[S13]	6.9	15 bar
f-CNT-M (M=La_2O_3, Ni)[S15]	6.2%	100
$Ti(OC_3H_7)_4$ @MgH_2	5.2%	
MgH_2-(CuO)@Gr[S11]	6.1%	290
This work	7.0%	<200

Table S2. The sorption temperature and content of hydriding and dehydriding corresponding to several samples.

Sample	H_2 absorb/desorption temperature (°C)	H_2 content/Time(min)
catalyst-5 wt%@MgH_2	200/200	6.8/60
catalyst-10 wt%@MgH_2	200/200	6.8/30
catalyst-30 wt%@MgH_2	200/200	6.8/10
catalyst-50 wt%@MgH_2	200/200	6.8/10

3. Reference

S1 S. Kiruthika, H. Fjellvåg, P. Ravindran, Amphoteric behavior of hydrogen (H^{+1} and H^{-1}) incomplex hydrides from van der Waals interaction including ab initio calculations, J. Mater. Chem. A., 2019, **7**, 6228-6240.

S2 C. Lu, Y. L. Ma, F. Li, H. Zhu, X. Q. Zeng, W. J. Ding, J. B. Wu, T. Deng, J. X. Zou, Visualization of fast "hydrogen pump" in core-shell nanostructured Mg@Pt through hydrogen stabilized Mg_3Pt, J. Mater. Chem. A., 2019, **7**, 14629-14637.

S3 Y. Li, M. H. Chen, B. Liu, Y. Zhang, X. Q. Liang, X. H. Xia, Heteroatom Doping: An Effective way to boost sodium Ion storage, Adv. Energy Mater., 2020, **10**, 2000927.

S4 N. Balahmar, R. Mokaya, Oxygen-rich microporous carbons with exceptional hydrogen storage capacity, Nat. Commun., 2017, **8**, 1545.

S5 K. J. Jeon, H. R. Moon, A. M. Ruminski, B. Jiang, C. Kisielowski, R. Bardhan, J. J. Urban, Air-stable magnesium nanocomposites provide rapid and high-capacity hydrogen storage without using heavy-metal catalysts, Nat. Mater., 2011, **10**, 286-90.

S6 J. X. Zou no cages by titanium do, H. Guo, X. Q. Zeng, S. Zou, X. Chen, W. J. Ding, Hydrogen storage properties of Mg-TM-La (TM=Ti, Fe, Ni) ternary composite powders prepared through arc plasma method, Int. J. Hydrogen.energ., 2013, **38**, 8852-8862.

S7 J. X. Zou, X. Q. Zeng, Y. J. Ying, X. Chen, H. Guo, S. Zou, W.J. Ding, Study on the hydrogen storage properties of core-shell structured Mg-RE (RE=Nd, Gd, Er) nano-composites synthesized through arc plasma method, Int. J. Hydrogen.energ., 2013, **38**, 2337-2346.

S8 R. Y. Li, Y. Wang, Modification of boron nitride naping results unexpectedly in exohedral complexes, Nat. Commun., 2019, **10**, 4908.

S9 S. K. Pandey, S. K. Verma, A. Bhatnagar, T. P. Yadav, Catalytic characteristics of titanium-(IV)-isopropoxide (TTIP) on de/re-hydrogenation of wet ball-milled MgH_2/Mg., Int J Energy Res., 2022, **46**, 17602–17615.

S10 H. Liang, D. D. Chen, W. J. Li, M. F. Chen, R. Snyders, Study of the synthesis of PMMA Mg nanocomposite for hydrogen storage application, Int. J. Hydrogen. energ., 2020, **45**, 4743-4753.

S11 V. Shukla, T. P. Yadav, Notable catalytic activity of CuO nanoparticles derived from metal-organic frameworks for improving the hydrogen sorption properties of MgH2, Int J Energy Res. 2022, **46**, 12804–12819.

S12 H. Liang, H. Zhang, Y. Zong, H. Xu, J. Luo, X. J. Liu, J. Xu, Studies of Ni-Mg catalyst for stable high efficiency hydrogen storage, J. Alloy. Compd., 2022, **905**, 164279.

S13 H. Liang, B. L. Cao, J. X. Zhu, X. H. Shen, M. Y. Zhu, B.Z. Geng, P. F. Zhang, S. L. Zhu, F. Y. Yu, R. Zhang, H. Tang, Q. Q. Yuan, J. Li, W.J. Li, Y. Chen, Intercalation optimized hexagonal boron nitride nanosheets for high efficiency hydrogen storage, Appl. Surf. Sci., 2022, **604**, 154118.

S14 H. Liang, J. Li, X. H. Shen, B. L. Cao, J. X. Zhu, B. Z. Geng, S. H. Zhu, W. J. Li, The study of amorphous La@Mg catalyst for high efficiency hydrogen storage, Int. J. Hydrogen Energ., 2022, **47**, 18404-18411.

S15 H. Liang, X. H. Du, J. Li, L. M. Sun, M. Song, W. J Li, Manipulating active sites on carbon nanotube materials for highly efficienthydrogen storage., 2023, **619**, 156740.